

Critical End Point of QCD Phase-Diagram: A Schwinger-Dyson Equation Perspective

Adnan Bashir
Michoacán University,
Mexico

Collaborators:
E. Guadalupe Gutiérrez, A Ahmad,
A. Ayala, A. Raya, J.R. Quintero

II Workshop on Perspectives in Non Perturbative QCD
May 12-13, 2014

Contents

- Introduction
- QCD at Zero Temperature

Chiral Symmetry Breaking

Confinement

Light Quark Flavors and Interaction Strength

- QCD at Finite Temperature and Chemical Potential

Propagators and Vertices

Chiral Symmetry Restoration

- Concluding Remarks

Introduction

Hadron Physics

QCD F
Diagram

Magnetic
Catalysis(α, eB)

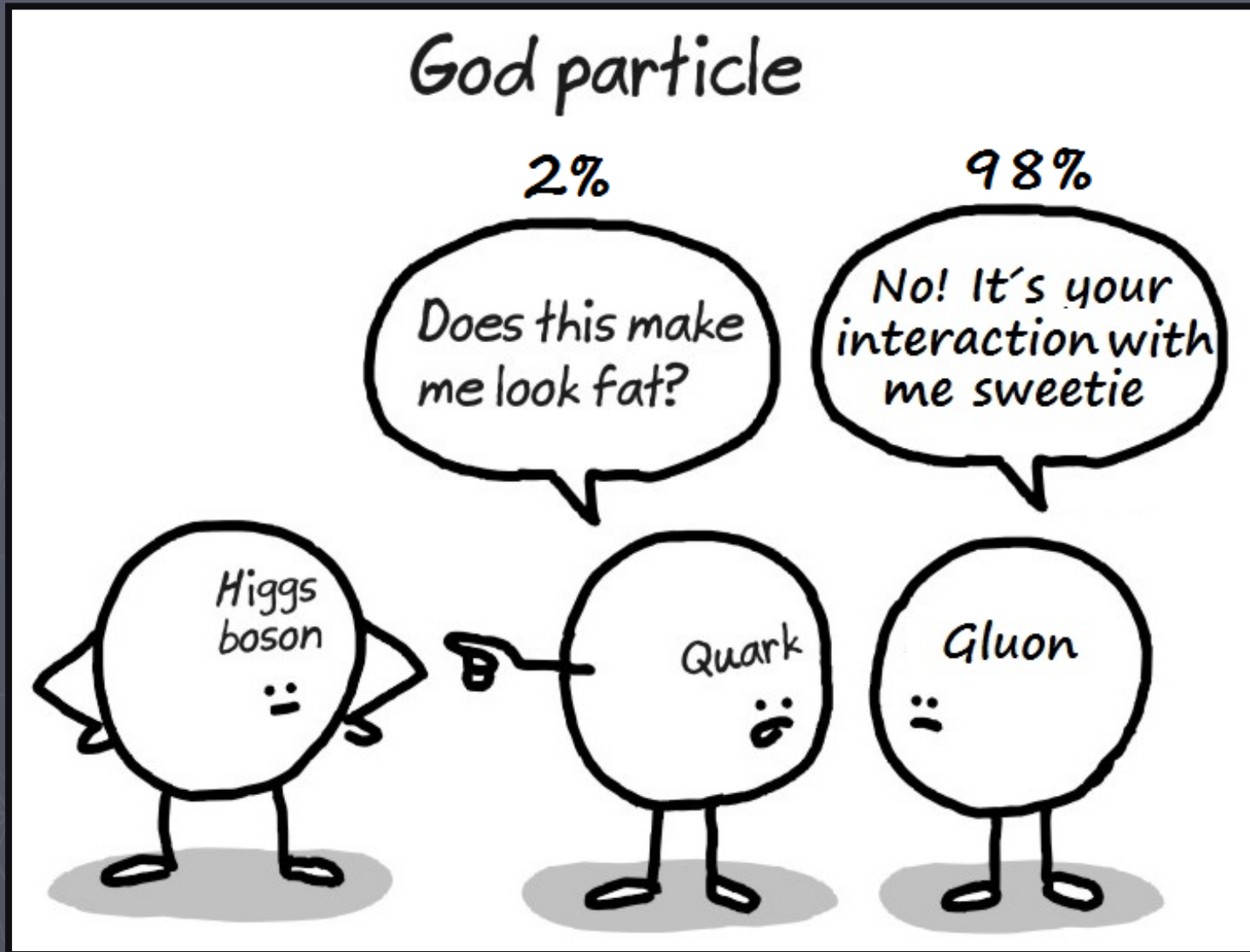
Running
Quark
Mass (α, N_f)

Chiral
Symmetry
Breaking

Condensed
Matter
Systems
(x, v_F, κ)

Schwinger-Dyson
Equations

QCD at Zero Temperature



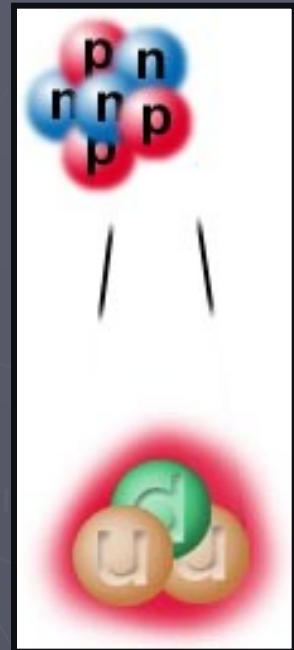
QCD at Zero Temperature

The QCD Lagrangian:

$$\mathcal{L} = -\frac{1}{4} F_{\alpha\beta}^A F_A^{\alpha\beta} + \sum_{\text{flavours}} \bar{q}_a (i\cancel{D} - m)_{ab} q_b$$

The diagram illustrates the QCD Lagrangian components. The first term, $-\frac{1}{4} F_{\alpha\beta}^A F_A^{\alpha\beta}$, is represented by a gluon-gluon vertex where two red wavy lines (gluons) meet at a black dot, with a downward-pointing arrow indicating the flow of momentum. The second term, involving quarks, is shown as a quark-gluon vertex where a blue line (quark) and a red wavy line (gluon) meet at a black dot, with a downward-pointing arrow indicating the flow of momentum. A horizontal blue arrow below the vertex indicates the direction of the quark's motion.

QCD at Zero Temperature



1000 MeV



5 MeV



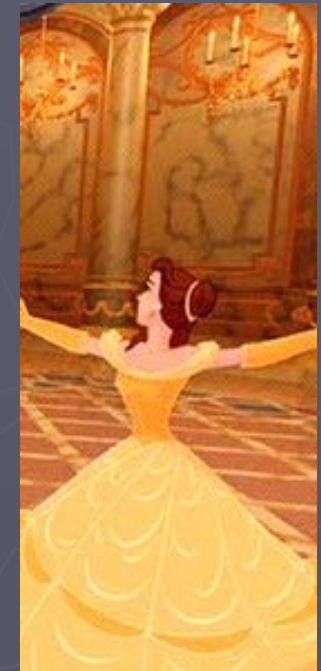
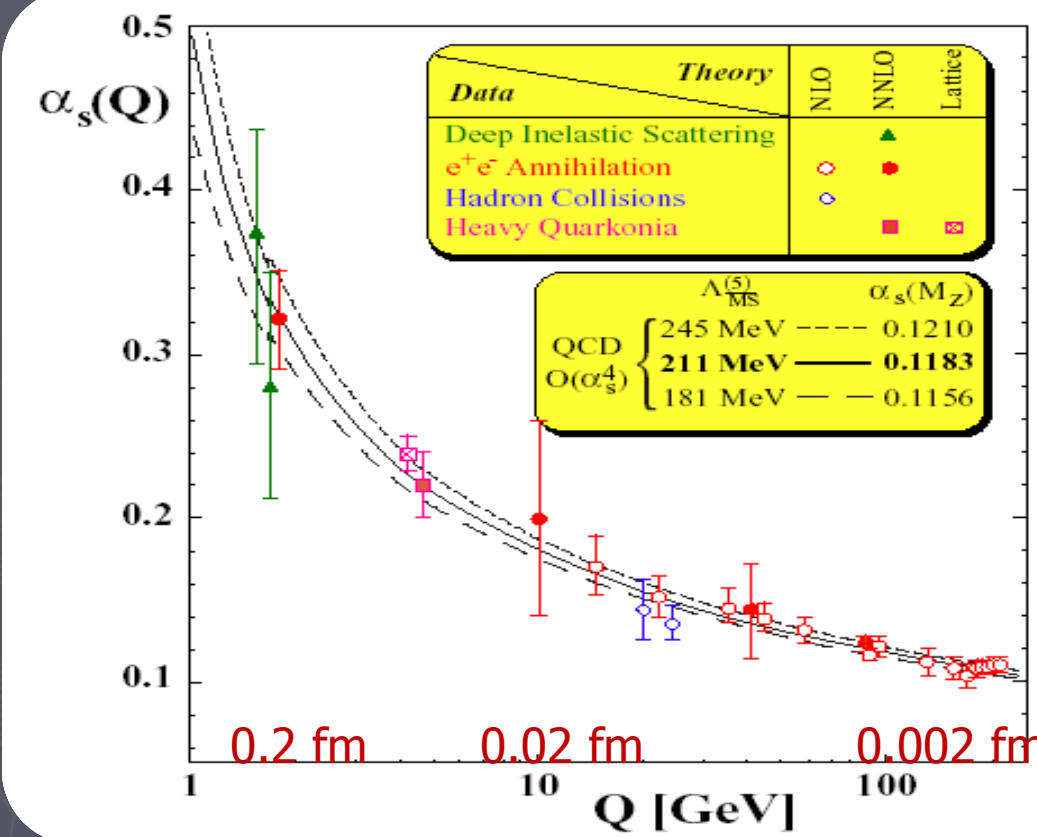
We can trace the origin of 98% of the luminous matter to QCD interactions.

QCD

QCD at Zero Temperature



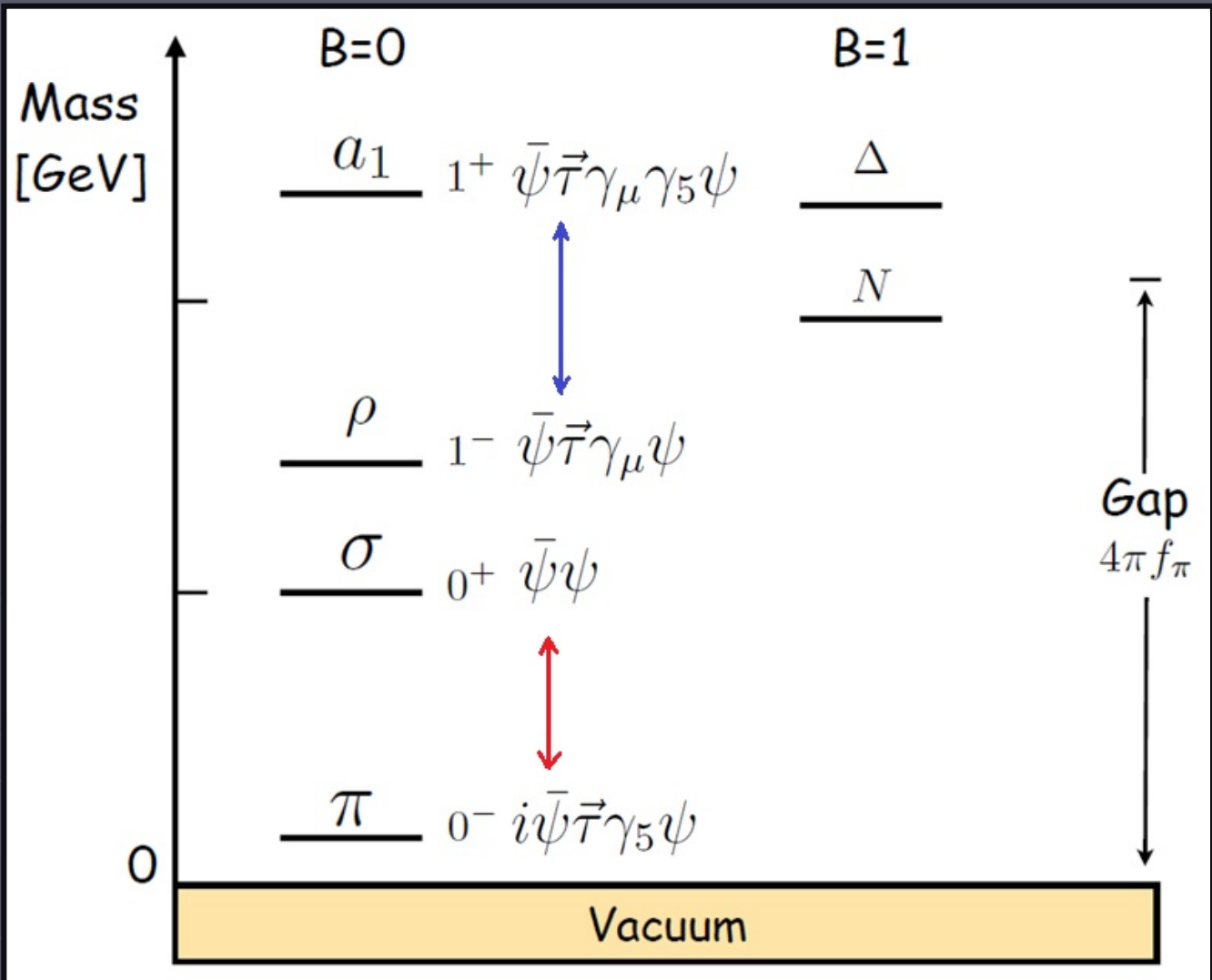
Infrared Increase



Asymptotic Freedom

QCD at Zero Temperature

Parity
Partners &
Chiral
Symmetry
Breaking



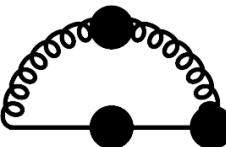
QCD at Zero Temperature

The quark propagator:

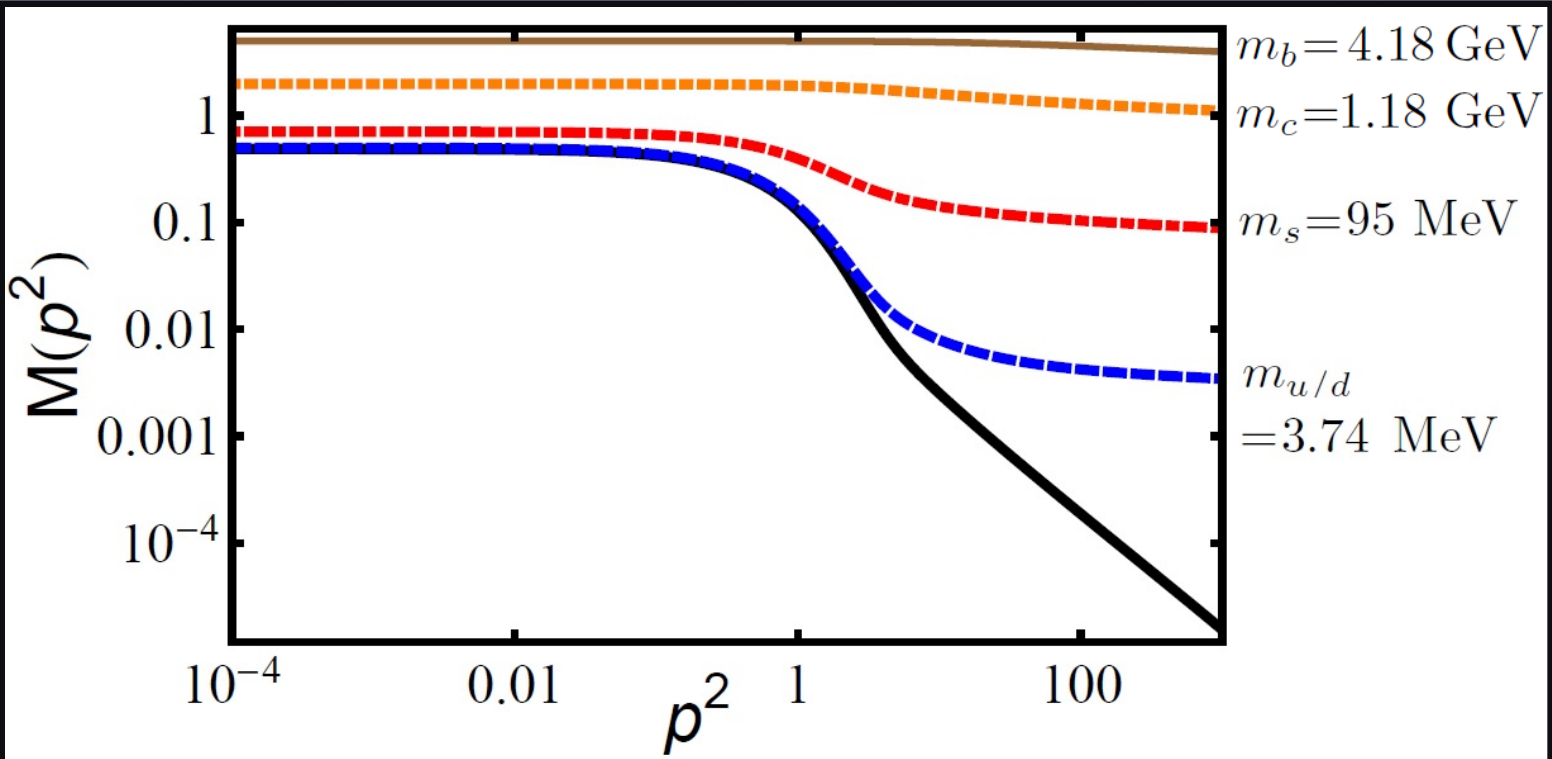
$$S(p^2, \mu^2) = i \gamma \cdot p A(p^2, \mu^2) + B(p^2, \mu^2) = \frac{Z(p^2, \mu^2)}{i \gamma \cdot p + M(p^2)}$$

-1

-1



Enhanced infrared
Effective interaction



QCD at Zero Temperature

Confinement: Can be inferred from the analytic properties of the propagator.

Violation of the axiom of reflection positivity

Schwinger
function

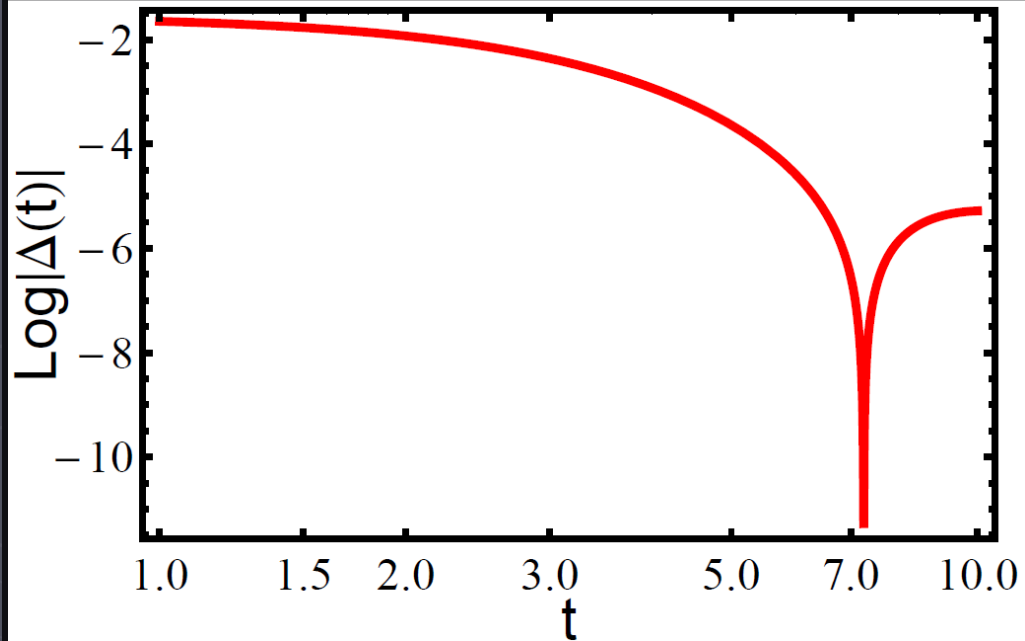
$$\Delta(t) = \int d^3x \int \frac{d^4p}{(2\pi)^4} e^{i(p_4 t + \mathbf{p} \cdot \mathbf{x})} \sigma_s(p^2)$$

stable asymptotic state

$$\Delta(t) \sim e^{-mt}$$

two complex conjugate mass-like singularities
 $\mu = a \pm ib$

$$\Delta(t) \sim e^{-at} \cos(bt + \delta)$$

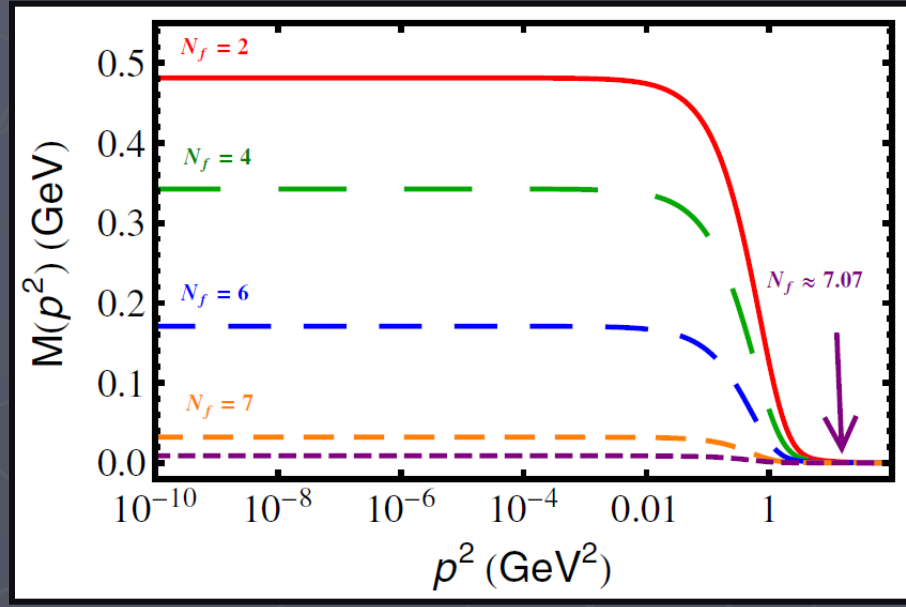
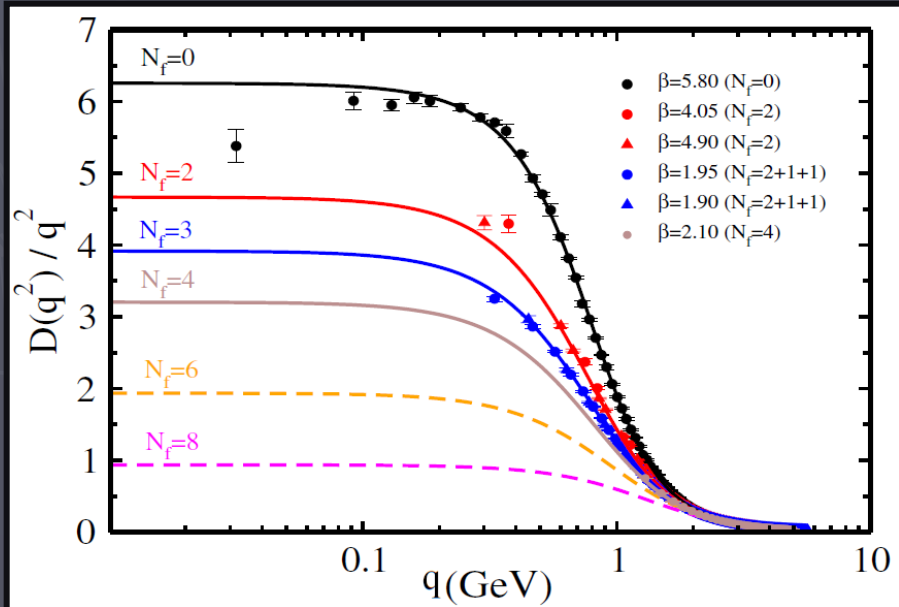


QCD at Zero Temperature

No. of light quark flavors also determine the extent of chiral symmetry breaking and confinement.

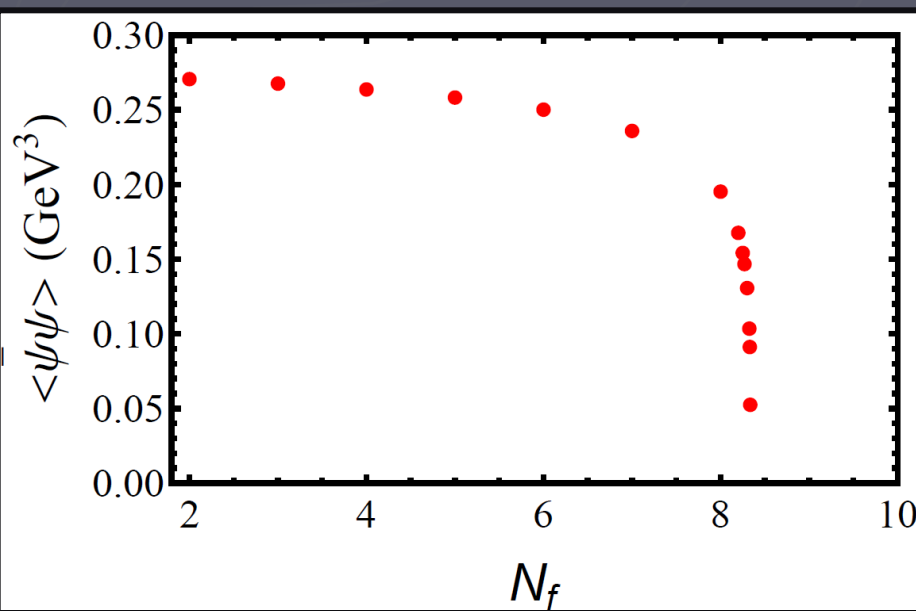
$$\Delta_{\mu\nu}^{ab}(q) = \delta^{ab} D(q^2) \left(\delta_{\mu\nu} - \frac{q_\mu q_\nu}{q^2} \right)$$

$$S(p) = \frac{Z(p^2)}{i\gamma \cdot p + M(p^2)}$$

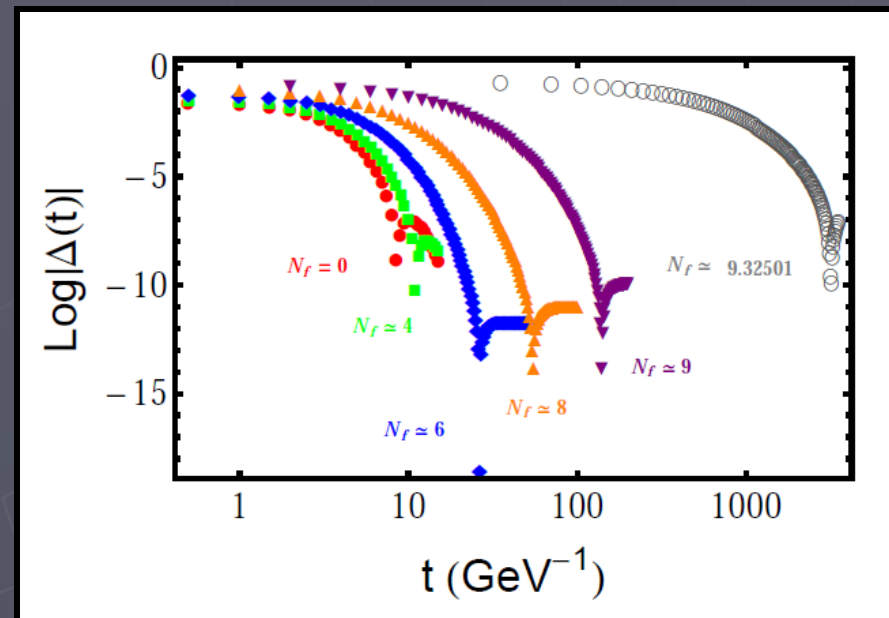


QCD at Zero Temperature

Increasing no. of light quark flavors restores chiral symmetry and triggers deconfinement.

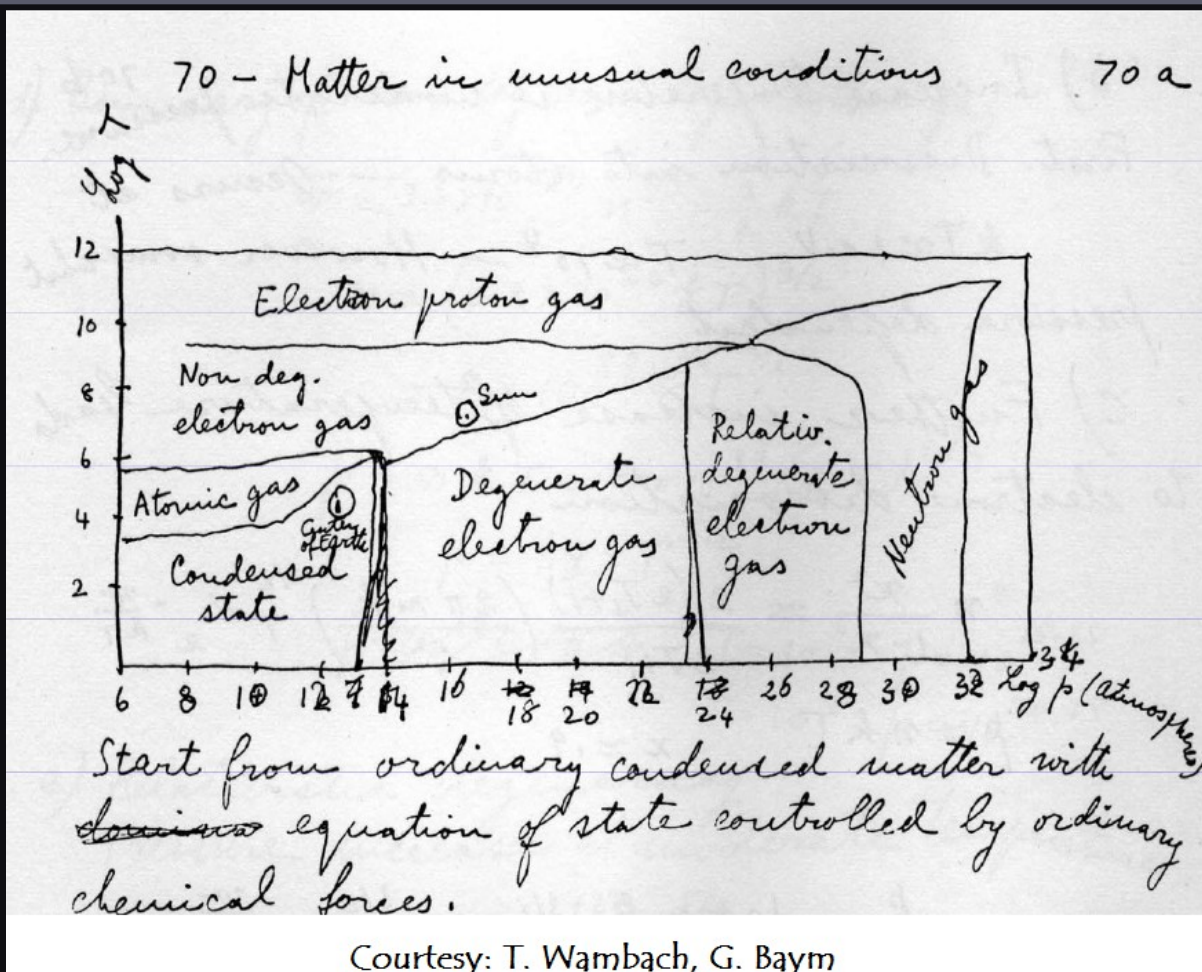


Chiral condensate



Confinement

QCD at Finite Temperature

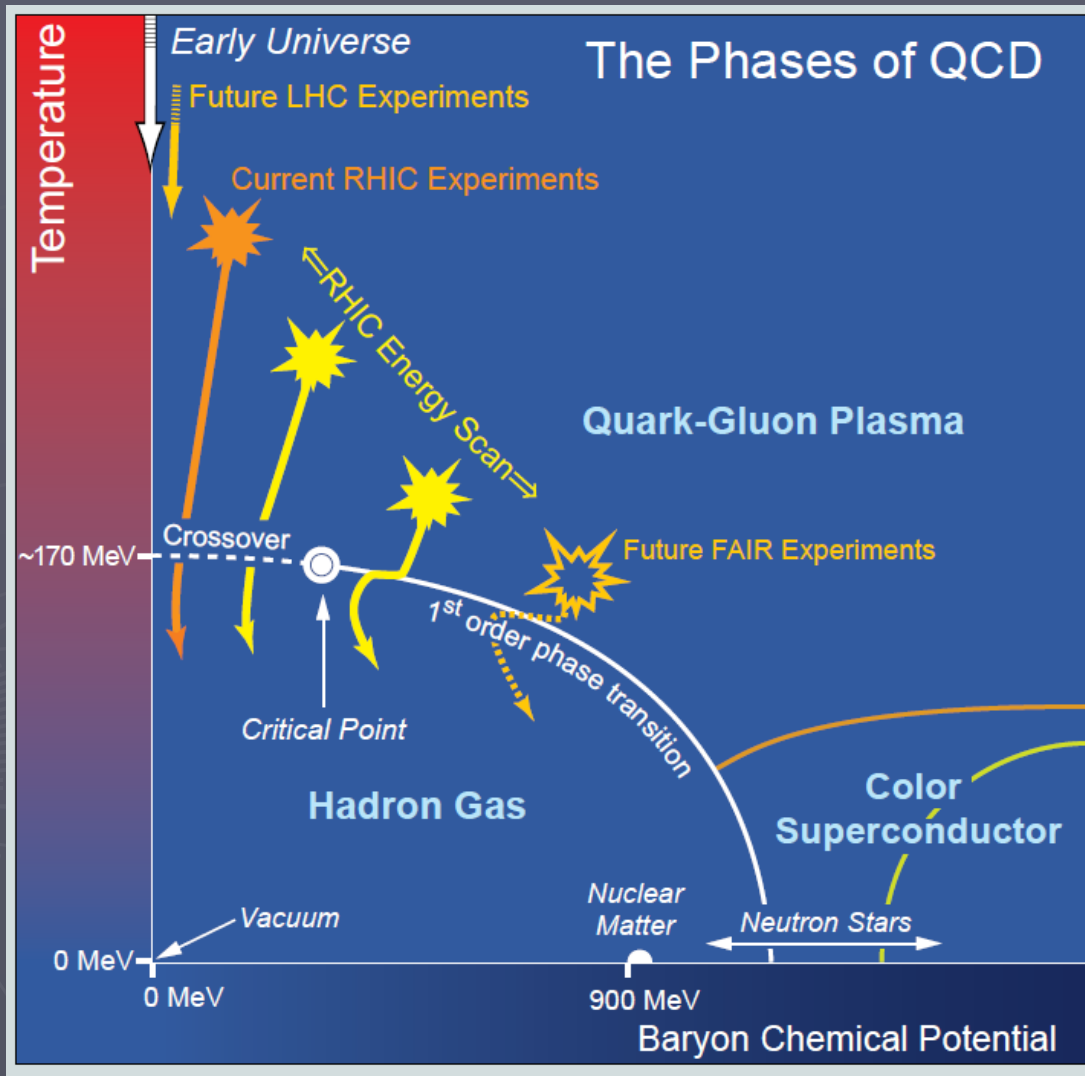


Fermi: Notes on Statistics and Thermodynamics (1953).

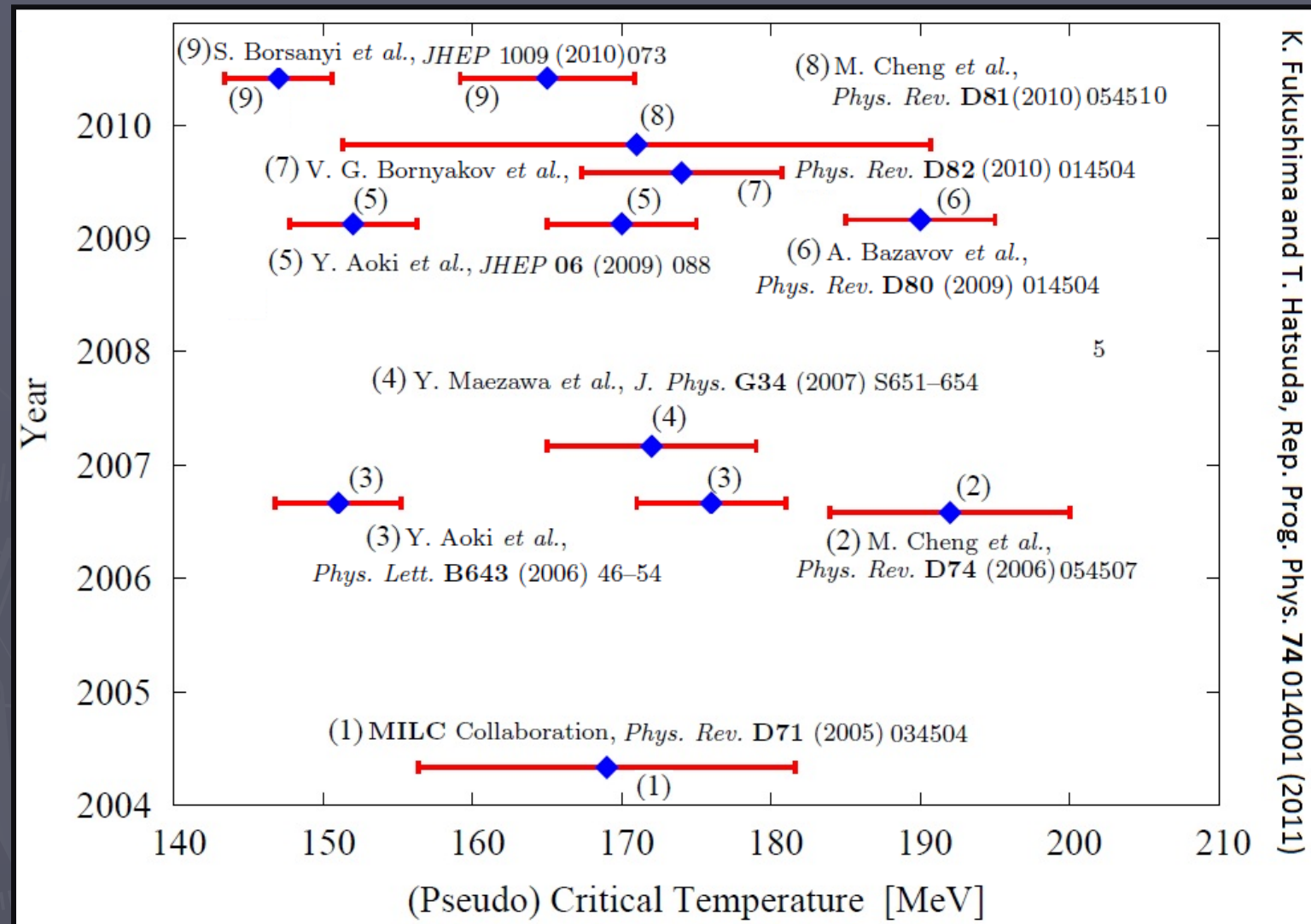
QCD at Finite Temperature

1. Relativistic Heavy-Ion Collider (RHIC) at Brookhaven National Laboratory (BNL)
2. Large Hadron Collider (LHC) at CERN
3. Heavy-Ion Collider HIC at RHIC
4. Facility for Antiproton and Ion Research (FAIR) at GSI
5. Nuclotron-based Ion Collider Facility (NICA) at JINR
6. Japan Proton Accelerator Research Complex (J-PARC) at JAERI

QCD at Finite Temperature



QCD at Finite Temperature



K. Fukushima and T. Hatsuda, Rep. Prog. Phys. **74** 014001 (2011)

Some lattice result at $\mu=0$.

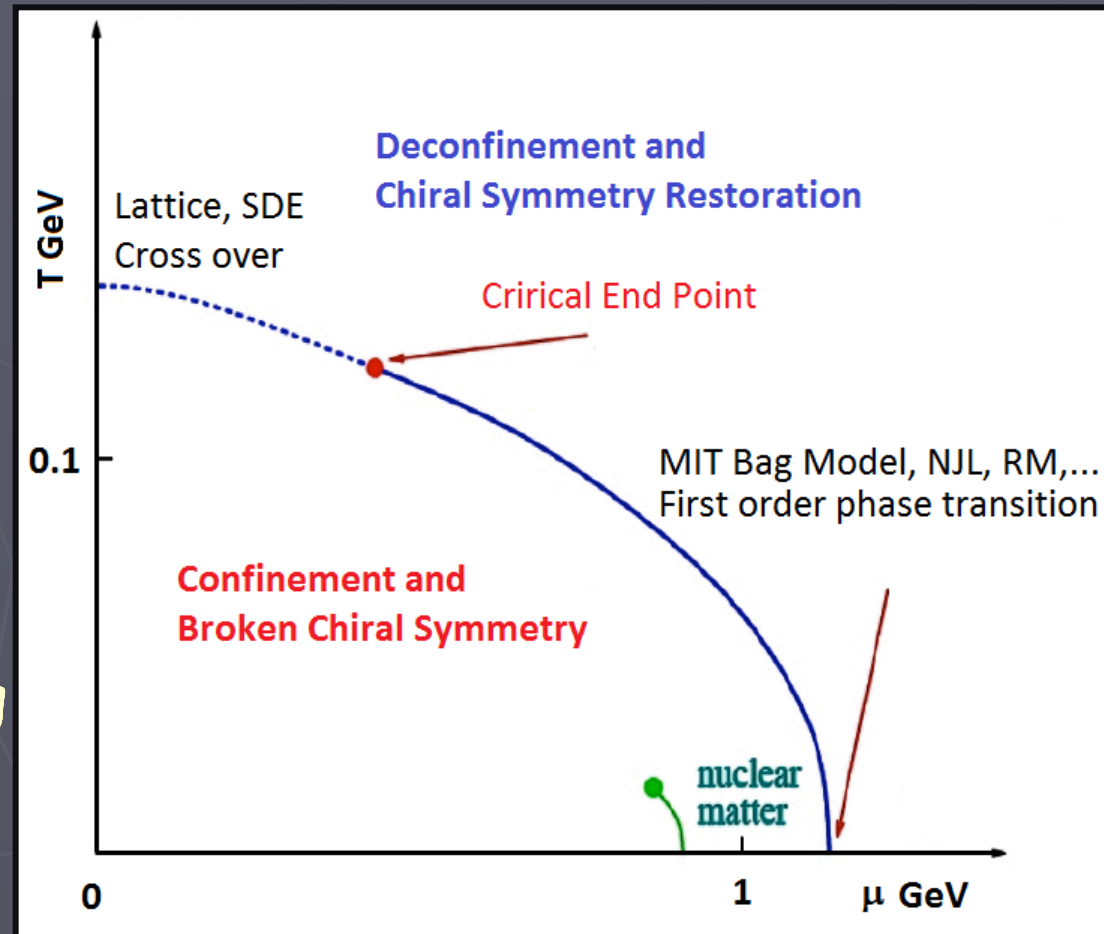
Facts and Challenges

The theory at the edges is better understood.

Lattice QCD and SDE find a rapid & smooth cross-over at large T and $\mu_B=0$.

Various models find a strong 1st order phase transition at large μ_B and $T=0$.

1st order line originating at $T=0$ cannot end at $\mu_B=0$ as it is a cross-over. There must exist A critical end point.



Facts and Challenges

A sound theoretical prediction for the existence and location of the critical end point on the QCD phase diagram is a challenging task.

Are the two phase transitions, corresponding to confinement and deconfinement & chiral symmetry breaking and its restoration, coincidental?

As they both owe themselves to the diminishing of the QCD interaction strength, one may expect them to chart out the same curve in the QCD phase diagram.

AB, A. Raya, I.C. Cloet, C.D. Roberts, Phys. Rev. C78 055201 (2008) [QED3, N_f]

AB, A. Raya, J. Rodríguez, Phys. Rev. D88 054003 (2013) [QCD, N_f]

Schwinger-Dyson Equations

Charting out the phase diagram from the basic building blocks of QCD is an outstanding problem.

- Through SDEs, the fundamental equations of QCD, we can attack the problem through first principles in the continuum.

Schwinger-Dyson Equations combine the non-perturbative regime of a theory with its perturbative limit naturally.

Thus they provide an ideal frame-work to study the transition region in QCD phase diagram where non perturbative phenomena of chiral symmetry breaking and confinement melt away.

S-X Qin, L. Chang, H. Chen, Y-X Liu, C.D. Roberts, Phys. Rev. Lett. 106 172301 (2011)

C.S. Fischer, J. Luecker, Phys. Lett. B 718 1036 (2013)

Schwinger-Dyson Equations

Quark Propagator: At finite T and μ , its general form is:

$$S^{-1}(\vec{p}, \tilde{w}_n) = iA(\vec{p}^2, \tilde{w}_n^2)\vec{\gamma} \cdot \vec{p} + i\gamma_4 \tilde{w}_n^2 C(\vec{p}^2, \tilde{w}_n^2) + B(\vec{p}^2, \tilde{w}_n^2)$$
$$\tilde{w}_n = w_n + i\mu \text{ and } w_n = 2(n+1)\pi T$$

Its solution for the scalar functions A, B and C can be obtained by solving the SDE:

$$S^{-1}(\vec{p}, \tilde{w}_n) = i\vec{\gamma} \cdot \vec{p} + i\gamma_4 \tilde{w}_n + \Sigma(\vec{p}, \tilde{w}_n) \quad \text{← (Self Energy)}$$
$$\Sigma(\vec{p}, \tilde{w}_n) = T \sum_{l=-\infty}^{l=\infty} \int \frac{d^3 q}{(2\pi)^3} g^2 D_{\mu\nu}(\vec{p} - \vec{q}, \Omega_{nl}) \quad \text{← Gluon Propagator}$$
$$\times \frac{\lambda^a}{2} \gamma_\mu S(\vec{q}, \tilde{w}_l) \frac{\lambda^a}{2} \Gamma_\nu(\vec{q}, \tilde{w}_l, \vec{p}, \tilde{w}_n) \quad \text{← Quark-Gluon Vertex}$$

Schwinger-Dyson Equations

Gluon Propagator:

$$g^2 D_{\mu\nu}(\vec{k}, \Omega_{nl}) = P_{\mu\nu}^T D_T(\vec{k}^2, \Omega_{nl}) + P_{\mu\nu}^L D_L(\vec{k}^2, \Omega_{nl})$$

$$P_{\mu\nu}^L = \delta_{\mu\nu} - \frac{k_\mu k_\nu}{k^2} - P_{\mu\nu}^T, \quad P_{44}^T = P_{4i}^T = 0, \quad P_{ij}^T = \delta_{ij} - \frac{k_i k_j}{\vec{k}^2}$$

We follow the lead of Qin et. al.:

S. Qin, L. Chang, C.D. Roberts, Y.X. Liu, Phys. Rev. Lett. 172301 (2011)

$$D_T(\vec{k}^2, \Omega_{nl}^2) = \mathcal{D}(T) \frac{4\pi^2}{\sigma^6} (\vec{k}^2 + \Omega_{nl}^2) e^{-(\vec{k}^2 + \Omega_{nl}^2)/\sigma^2}$$

$$D_L(\vec{k}^2, \Omega_{nl}^2) = \mathcal{D}(T) \frac{4\pi^2}{\sigma^6} (\vec{k}^2 + \Omega_{nl}^2) e^{-(\vec{k}^2 + \Omega_{nl}^2 + m_g^2)/\sigma^2}$$

where $\sigma = 0.5$ GeV.

Schwinger-Dyson Equations

Quark-Gluon
Vertex:

Gauge Invariance Constraints:

$$\Gamma_\mu(P_1, P_2) = \Gamma_\mu^L(P_1, P_2) + \Gamma_\mu^T(P_1, P_2)$$

$$Q^\mu \Gamma_\mu^T(P_1, P_2) = 0, \quad \Gamma_\mu^T(P, P) = 0, \quad Q = P_1 - P_2$$

$\Gamma_\mu(P_1, P_2)$

Lorentz vectors: $\gamma_\mu, P_{1\mu}, P_{2\mu}$ and U_μ

Lorentz scalars: $1, \not{P}_1, \not{P}_2, \not{U}, \not{P}_1 \not{P}_2, \not{P}_1 \not{U}, \not{P}_2 \not{U}, \not{P}_1 \not{P}_2 \not{U}$

$$V_{1\mu} = P_{1\mu} \not{P}_1, \quad V_{2\mu} = P_{2\mu} \not{P}_2, \quad V_{3\mu} = P_{1\mu} \not{P}_2, \quad V_{4\mu} = P_{2\mu} \not{P}_1$$

$$V_{5\mu} = \gamma_\mu \not{P}_1 \not{P}_2, \quad V_{6\mu} = \gamma_\mu, \quad V_{7\mu} = P_{1\mu}, \quad V_{8\mu} = P_{2\mu}$$

$$V_{9\mu} = P_{1\mu} \not{P}_1 \not{P}_2, \quad V_{10\mu} = P_{2\mu} \not{P}_1 \not{P}_2, \quad V_{11\mu} = \gamma_\mu \not{P}_1, \quad V_{12\mu} = \gamma_\mu \not{P}_2$$

$$V_{13\mu} = V_{1\mu} \not{U}, \quad V_{14\mu} = V_{2\mu} \not{U}, \quad V_{15\mu} = V_{3\mu} \not{U}, \quad V_{16\mu} = V_{4\mu} \not{U}$$

$$V_{17\mu} = V_{5\mu} \not{U}, \quad V_{18\mu} = V_{6\mu} \not{U}, \quad V_{19\mu} = V_{7\mu} \not{U}, \quad V_{20\mu} = V_{8\mu} \not{U}$$

$$V_{21\mu} = V_{9\mu} \not{U}, \quad V_{22\mu} = V_{10\mu} \not{U}, \quad V_{23\mu} = V_{11\mu} \not{U}, \quad V_{24\mu} = V_{12\mu} \not{U}$$

$$V_{25\mu} = U_\mu, \quad V_{26\mu} = U_\mu \not{U}, \quad V_{27\mu} = U_\mu \not{P}_1, \quad V_{28\mu} = U_\mu \not{P}_2$$

$$V_{29\mu} = U_\mu \not{P}_1 \not{U}, \quad V_{30\mu} = U_\mu \not{P}_2 \not{U}, \quad V_{31\mu} = U_\mu \not{P}_1 \not{P}_2, \quad V_{32\mu} = U_\mu \not{P}_1 \not{P}_2 \not{U}$$

Schwinger-Dyson Equations

Quark-Gluon Vertex:

$$\begin{aligned}\Gamma_\mu^L(P_1, P_2) = & \gamma_\mu - \frac{1}{2}[a(P_1) + a(P_2)]\gamma_\mu - \frac{a(P_1) - a(P_2)}{2(P_1^2 - P_2^2)}(P_{1\mu} + P_{2\mu})(P_1 + P_2) \\ & - \frac{b(P_1) - b(P_2)}{(P_1^2 - P_2^2)}(P_{1\mu} + P_{2\mu})\not{U} + \frac{1}{2}[c(P_1) + c(P_2)]\gamma_\mu\not{U} \\ & + \frac{c(P_1) - c(P_2)}{2(P_1^2 - P_2^2)}(P_{1\mu} + P_{2\mu})(P_1 + P_2)\not{U} + \frac{d(P_1) - d(P_2)}{(P_1^2 - P_2^2)}(P_{1\mu} + P_{2\mu})\end{aligned}$$

Perturbative HTL constraints have been calculated in:

A. Ayala, AB, Phys. Rev. D64 025015 (2001)

We make a modest but practical ansatz:

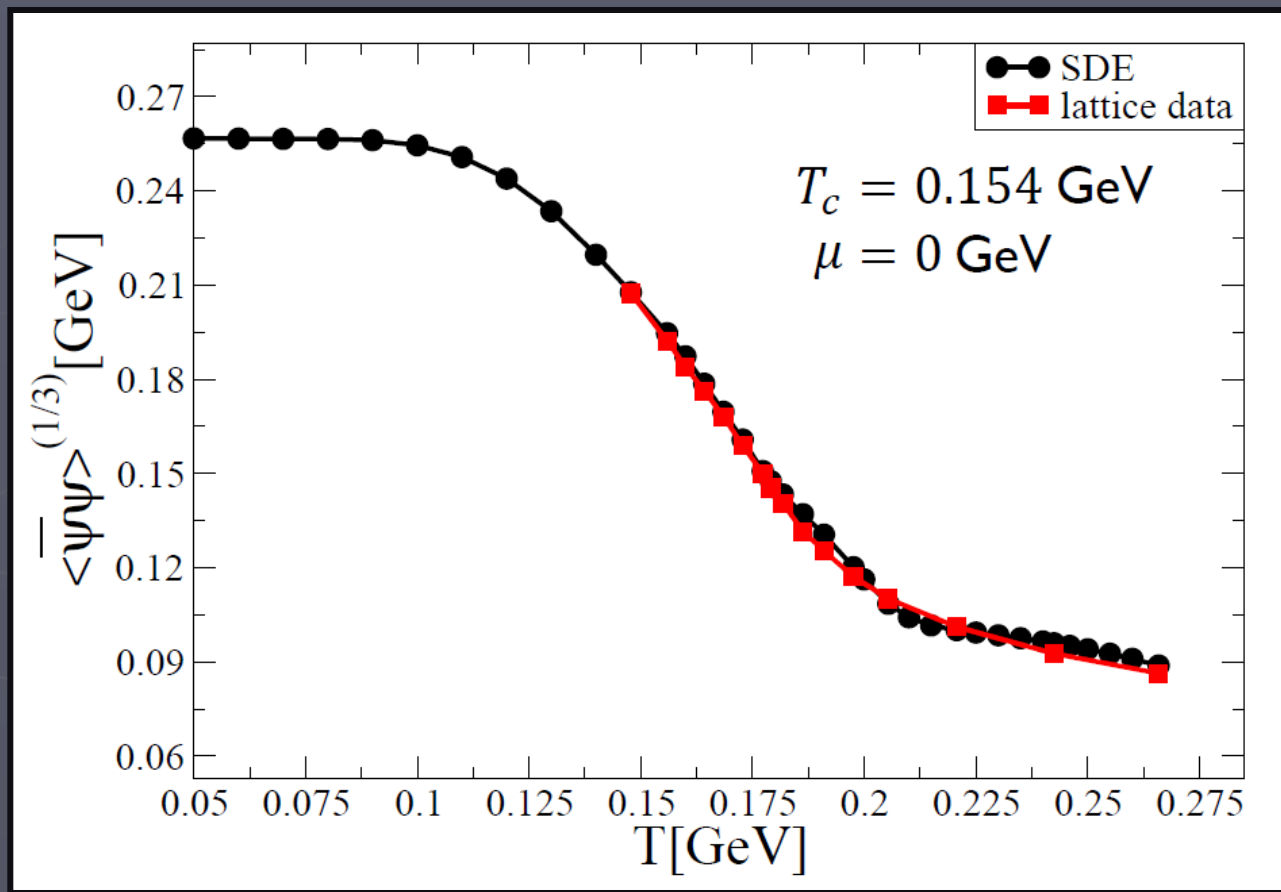
$$\mathcal{D}(T) \Gamma_\nu(\vec{q}, \tilde{w}_l, \vec{p}, \tilde{w}_n) = D(T) \gamma_\nu$$

and fix $D(T)$ to match lattice results along the $\mu=0$ axis.

Chiral Symmetry Restoration

$$\langle \bar{\psi} \psi \rangle = N_c T \sum_n \int \frac{d^3 q}{(2\pi)^3} \text{Tr}[S(\vec{q}, \tilde{w}_n)]$$

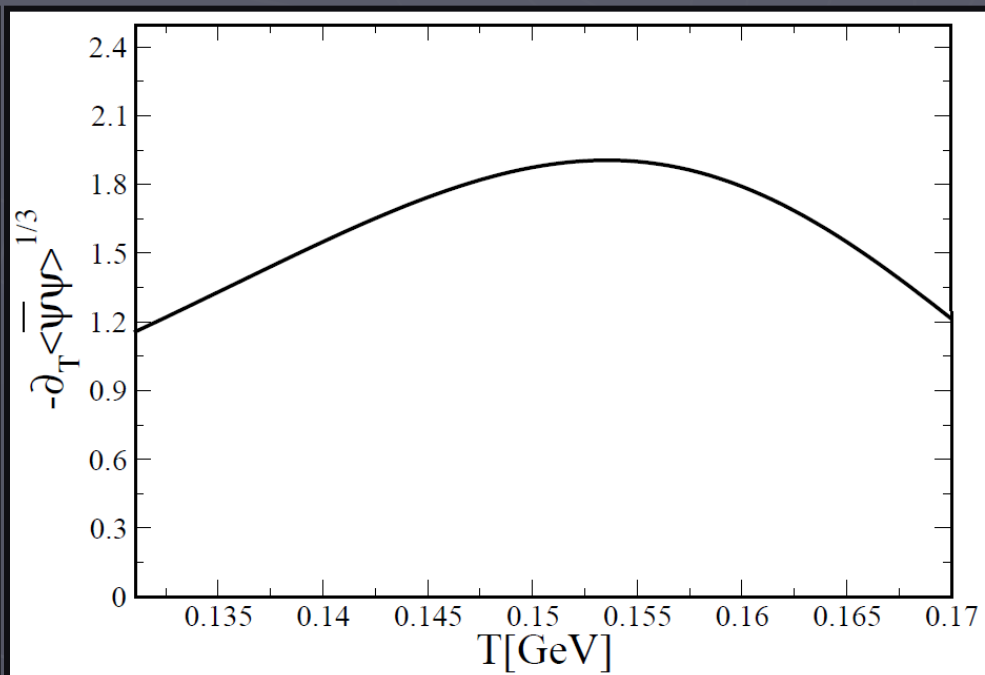
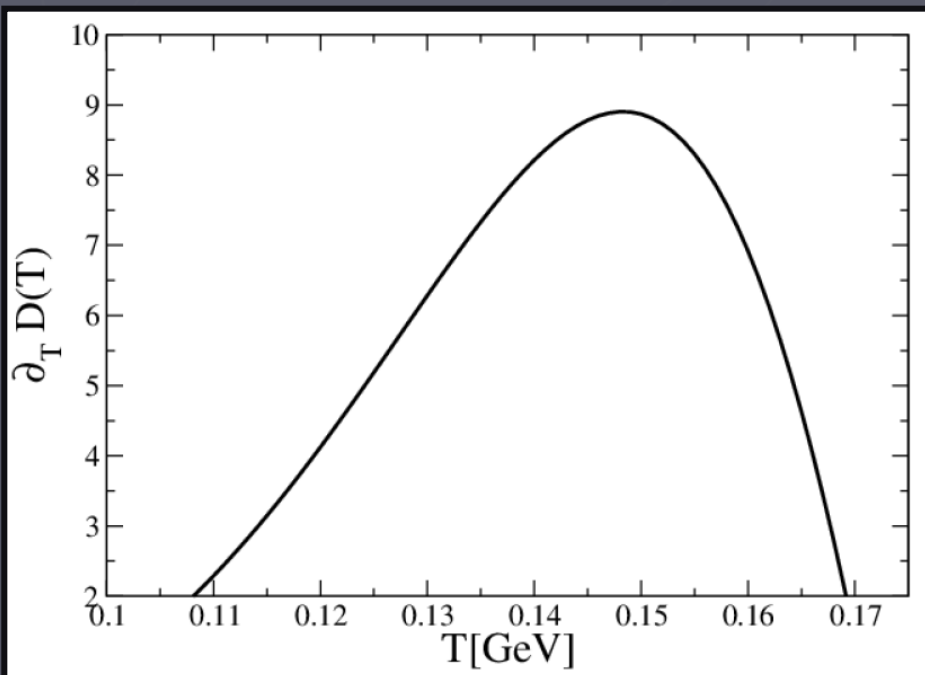
A. Bazavov et. al.,
Phys. Rev. D85
054503 (2012)



$D(T) = a - bT^3 - c \tanh(d - eT^3)$,
at $\mu = 0$ ($a = 2.17, b = 343.64, c = 1.76, d = 0.78$ and $e = 273.8$ with appropriate mass dimensions in GeV).

Chiral Symmetry Restoration

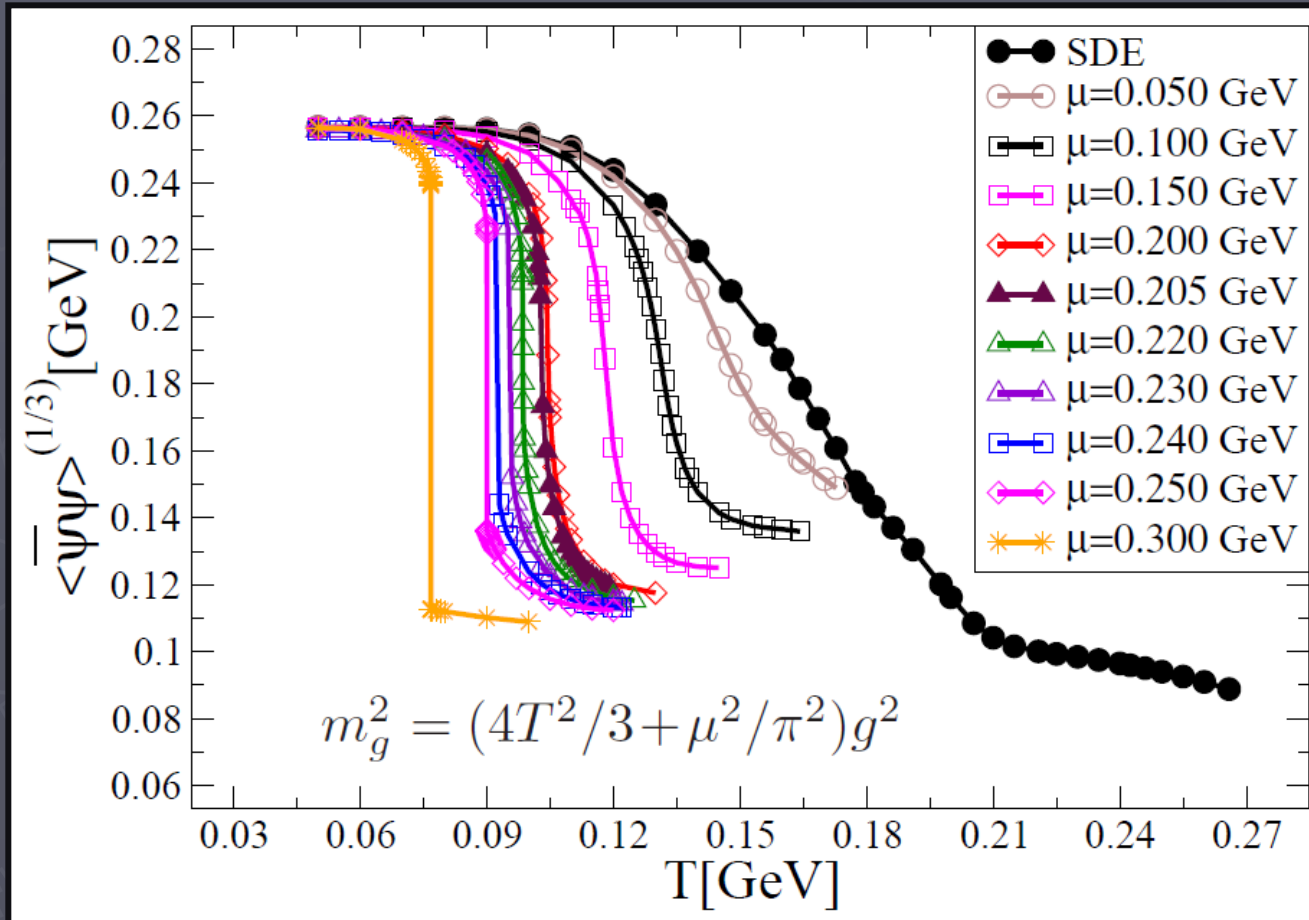
Chiral symmetry restoration also manifests itself in the function $D(T)$.



The critical temperature obtained from the behavior of $D(T)$ is 0.153 GeV whereas the obtained from the condensate is 0.154 GeV.

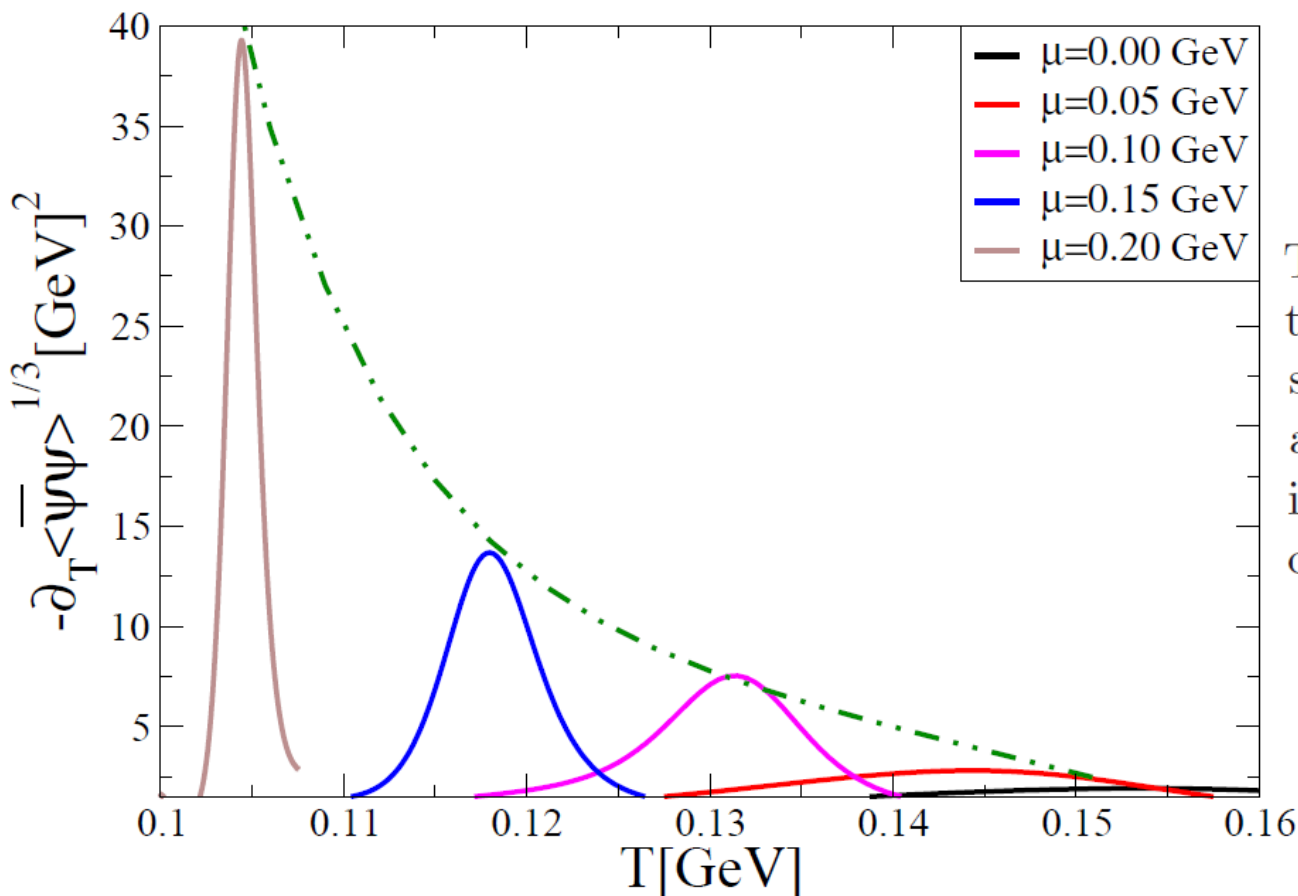
Chiral Symmetry Restoration

Knowing $D(T)$, we can repeat the exercise of computing the condensate off the $\mu=0$ axis.



Chiral Symmetry Restoration

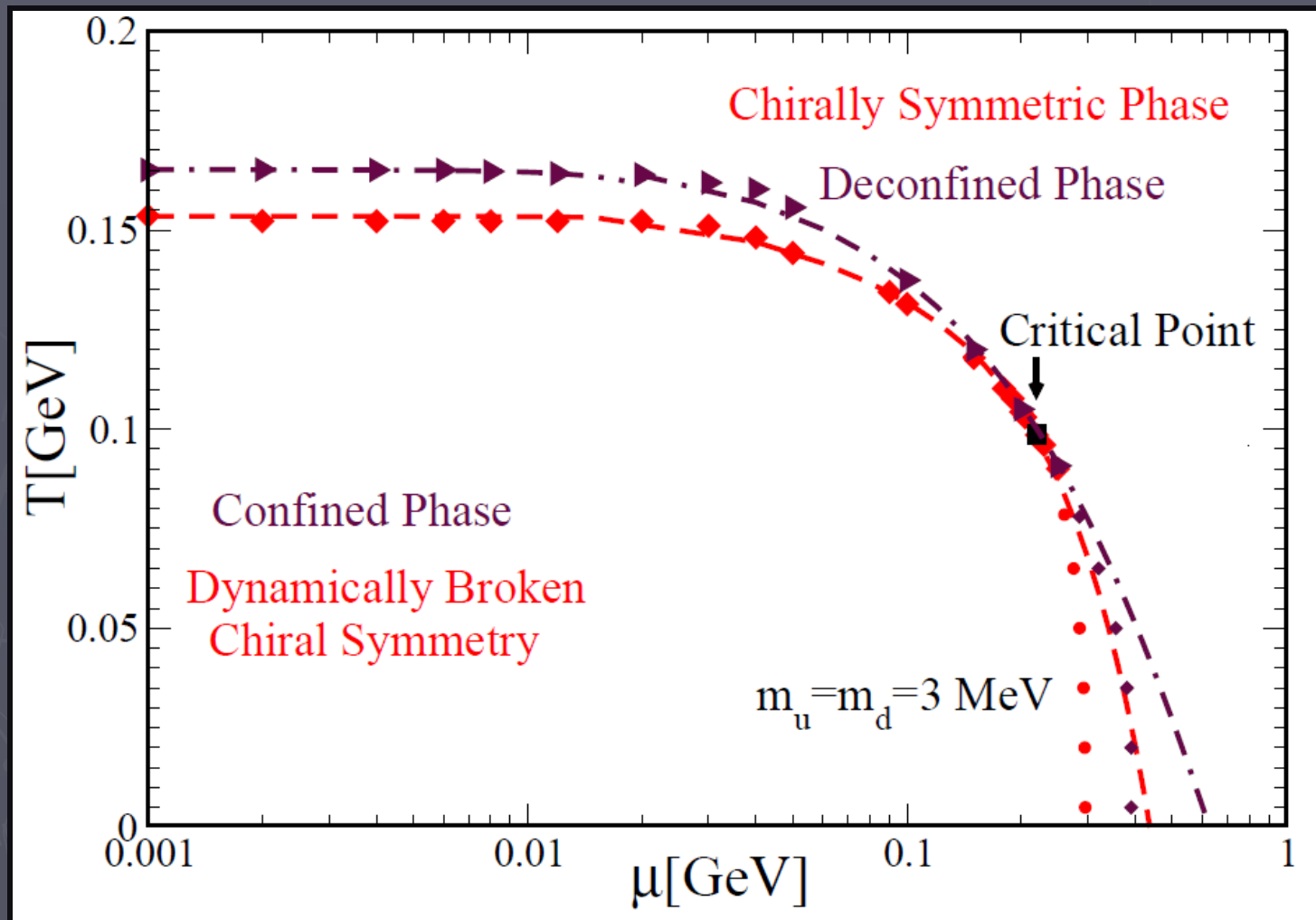
We plot our order parameter $-\partial_T \langle \bar{\psi} \psi \rangle$, and look at the plot for each μ . The maximum gives the pseudo critical point (T_c, μ_c) .



The height of this thermodynamic variable shoots up to *infinity* for a sufficiently large μ , indicating a change in the order of phase transition.

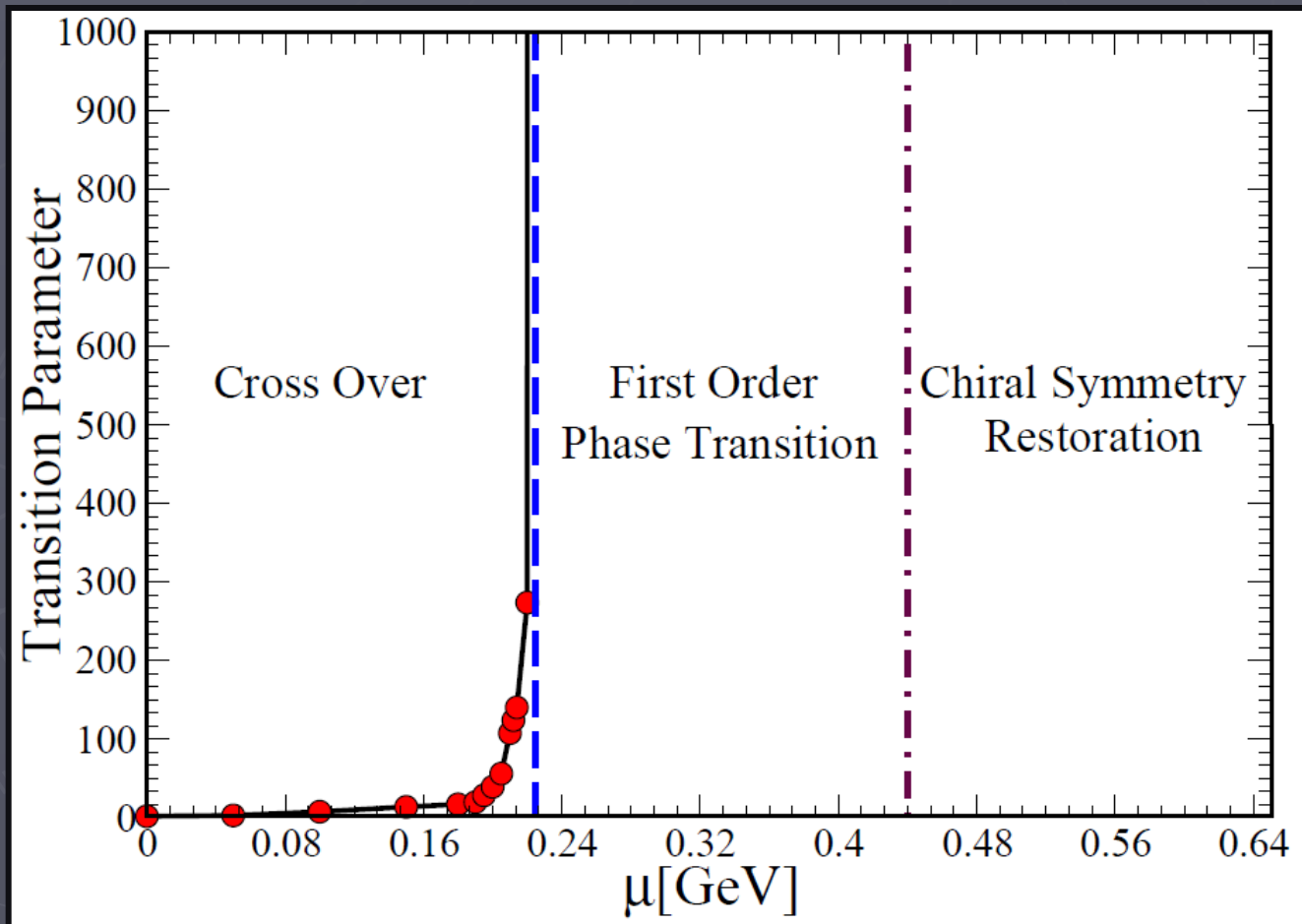
Chiral Symmetry Restoration

The critical line and the critical end point.



Chiral Symmetry Restoration

At chemical potential $\mu \sim 0.22$ GeV, the thermodynamic singularity arisen from disjointed condensate can be identified with the onslaught of 1st order phase transition.



Concluding Remarks

Exploiting the lattice results for the temperature evolution of the quark-anti-quark condensate, we use the Schwinger-Dyson equations to compute the same along the μ axis.

The temperature derivative of the quark-anti-quark condensate has a smooth and finite maximum for $\mu \sim 0$. As μ increases, this maximum starts growing and shoots up to infinity for $\mu \sim 0.22$ GeV. We identify this thermodynamic singularity with a change of the nature of phase transition from a simple cross-over to a 1st order phase transition.

Studying the analytic properties of the quark propagator, the confinement-deconfinement phase transitions appears to chart out the similar curve in the QCD phase diagram.